Figure S1

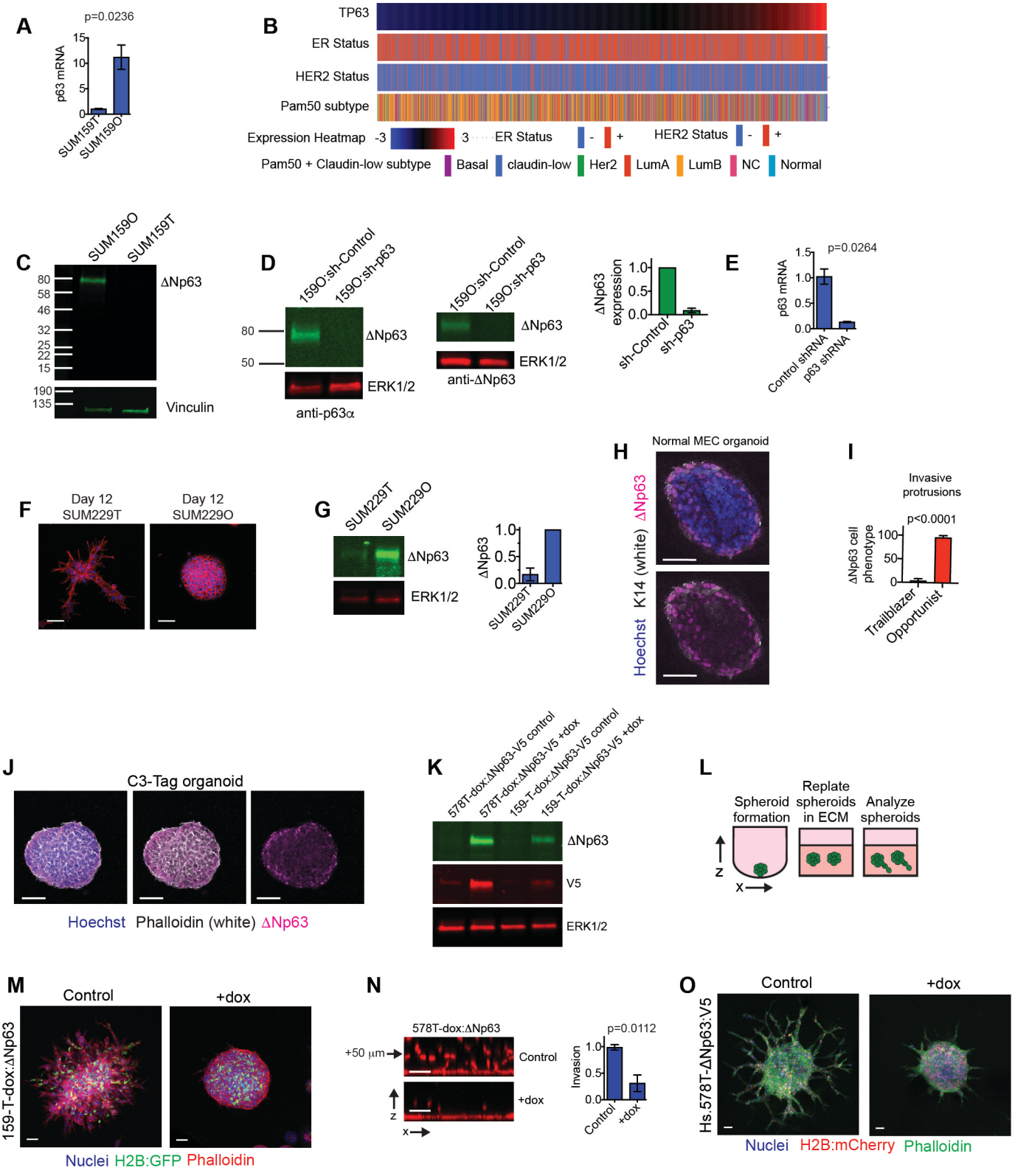

Continued on next page

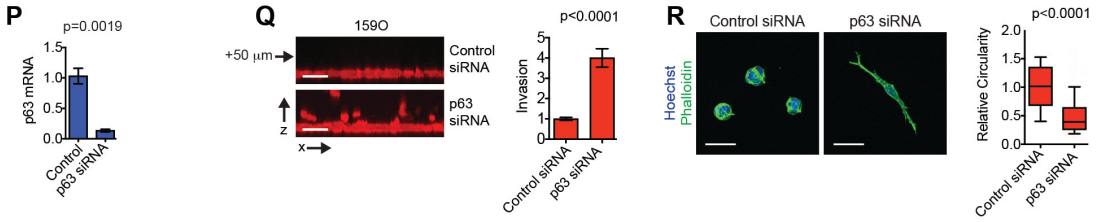

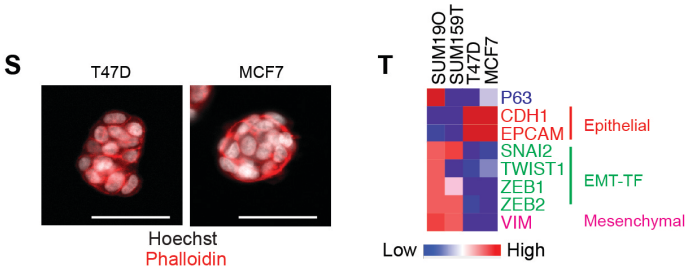

U

	Static epithelial	Opportunist EMT	Trailblazer EMT
ΔNp63	-	+	_
EMT-TF	-	+	+
Nonmotile	+	-	-
Motile	_	+	+
Invasive	_	-	+

Figure S1. (A) ΔNp63 mRNA expression in SUM159T and SUM159O cells determined by qPCR (mean±SEM, n=5). **(B)** p63 expression and corresponding ER status, HER2 status and PAM50 subtype in breast cancer patients from the METABRIC dataset. **(C)** Immunoblot showing the expression of ΔNp63 using a ΔNp63 specific antibody. Vinculin expression serves as a loading control. **(D)** An anti-p63α antibody detects p63 protein at the same molecular weight as the ΔNp63 antibody in **C.** The expression of ΔNp63 is depleted by p63 shRNA that targets all p63 isoforms, and is detected by the anti-p63α and anti-ΔNp63 antibodies. **(E)** qPCR results showing p63 depletion by a p63 targeting shRNA. Mean ±SEM (n=3). **(F)** SUM229 trailblazer (T) and opportunist (O) spheroids grown for 12 days in 3D culture and stained with phalloidin are shown (n=3). Scale bars, 50 µm. **(G)** Immunoblot shows ΔNp63 expression in SUM229T and SUM229O cells. Graph shows quantification of ΔNp63 expression (mean±standard deviation (SD) n=3). **(H)** ΔNp63 expression in mammary epithelial organoids. Scale bar, 50 µm. **(I)** Graph shows quantification of the phenotypes of ΔNp63 expressing cells in multicellular protrusions as a percentage of total organoids (mean ± SD, n=4 mice). A total of 32 multicellular protrusions were analyzed. **(J)** ΔNp63 expression at the interface with the ECM in noninvasive C3-Tag organoids. Scale bars, 50 µm. **(K)** Immunoblots showing doxycycline (dox) induced expression of V5-tagged ΔNp63 in 578T and SUM159T cells. **(L)** Graphic shows how clusters were formed by plating cells in low-adhesion plates for 24 h before plating in organotypic culture for 72 h. **(M)** Images show how dox induced ΔNp63 expression influences the invasion of clustered SUM159T spheroids. Scale bars, 50 µm. **(N)** x-z projections and quantification showing how doxycycline induced ΔNp63 influences 578T cell invasion (mean ± SD, n=3). Arrow is 50 µm above the monolayer and indicates invading cells. **(O)** Images show how dox induced ΔNp63 expression influences the invasion of clustered 578T spheroids. Scale bars, 50 µm. **(P)** qPCR results showing p63 depletion by a p63 targeting shRNA and siRNA pool (mean±SD, n=5. **(Q)** x-z projections and quantification showing how p63 siRNAs influences SUM159O invasion (mean±SD, n=12, r=3). Arrow is 50 µm above the monolayer and indicates invading cells. Scale bars, 50 µm. **(R)** Images show how p63 siRNAs influence the phenotype of SUM159O cells cultured on ECM for 24 h. Scale bars, 50 µm. Box and whisker plots (10-90 percentile). Control siRNA (n=1084 spheroids) and p63 siRNA (n=817 spheroids). **(S)** Images of spheroids formed by luminal-type estrogen receptor positive T47D and MCF7 cells that lack endogenous ΔNp63 expression. Scale bars, 50 µm. **(T)** Heatmap showing expression of p63, canonical epithelial (CDH1 (E-cadherin), EpCAM) and EMT-TFs (SNAI2 (Slug), Twist1, ZEB1, ZEB2 and the canonical mesenchymal marker Vimentin). **(U)** Summary of features that distinguish static epithelial, opportunist EMT and trailblazer EMT states. P-values determined by two-tailed Student's t-test **(A, E, I, N)** or Mann-Whitney U test **(Q-R)**.

Figure S2

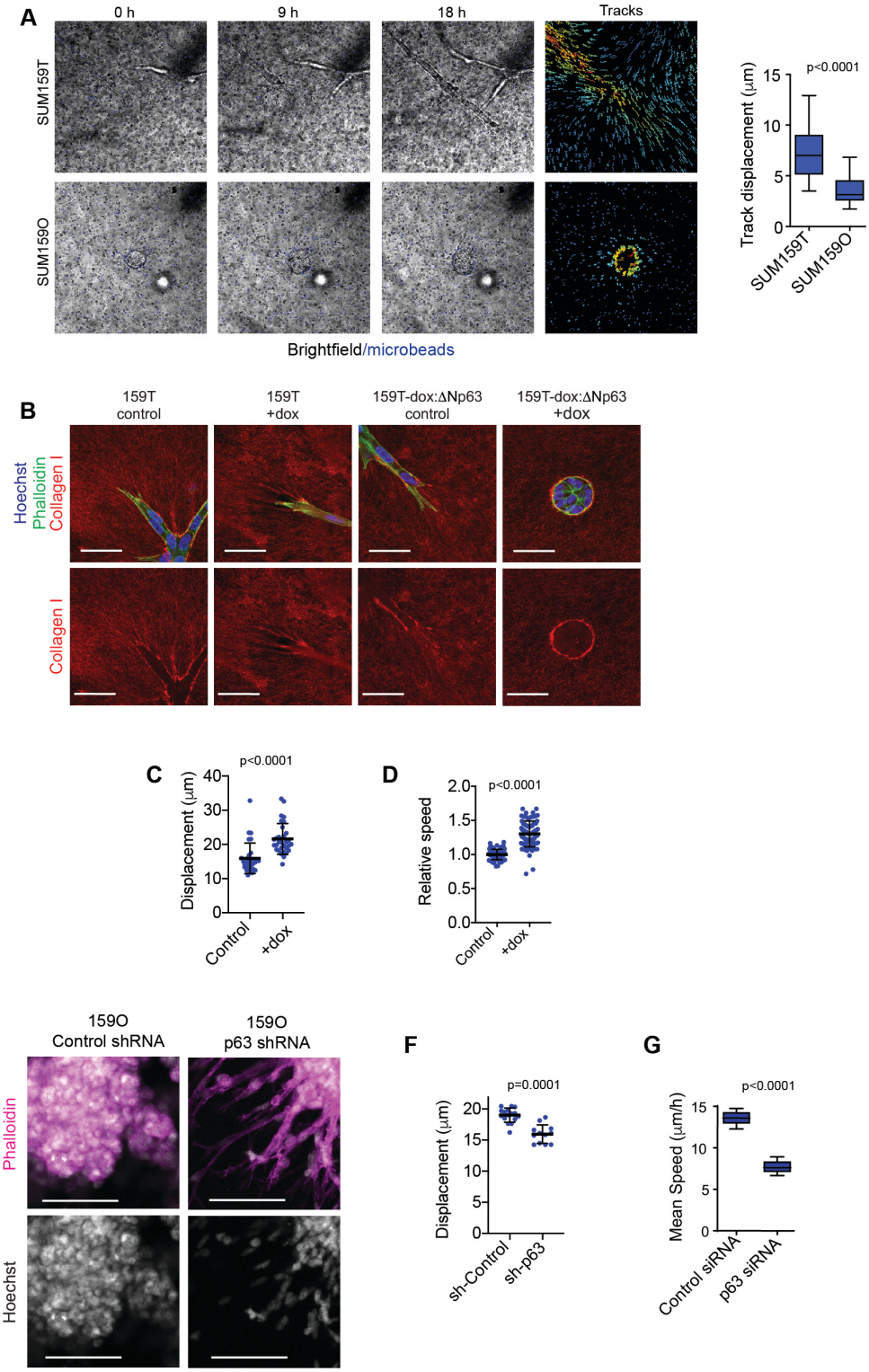
A
0 h
9 h
18 h
Tracks
SUM159T
SUM159O
Brightfield/microbeads
Track displacement (μm)
p<0.0001
SUM159T
SUM159O
B
159T control
159T +dox
159T-dox:ΔNp63 control
159T-dox:ΔNp63 +dox
Hoechst
Phalloidin
Collagen I
Collagen I
C
Displacement (μm)
p<0.0001
Control
+dox
D
Relative speed
p<0.0001
Control
+dox
E
159O Control shRNA
159O p63 shRNA
Hoechst
Phalloidin
Hoechst
F
Displacement (μm)
p=0.0001
sh-Control
sh-p63
G
Mean Speed (μm/h)
p<0.0001
Control siRNA
p63 siRNA

Figure S2. (A) Time-lapse imaging showing how trailblazer and opportunist cells influence the displacement of fluorescent microbeads in the surrounding ECM. Box and whisker plot (10-90 percentile). 159T (n=33 fields of view) and 159O (n=28 fields of view). P-values determined by Mann Whitney U test. **(B)** Images show how dox induced ΔNp63 expression influences the organization of Collagen I surrounding SUM159T spheroids in 3D culture. Scale bars, 50 μm. **(C)** Quantification shows the mean displacement of cells in control and dox induced ΔNp63 expressing SUM159T spheroids analyzed in **Fig. 2A-B**. Mean ±SD cell speeds for 30 spheroids for each condition. **(D)** Quantification shows how dox induced ΔNp63 influences the mean speed of 159T cells grown in 2D monolayers over 6 h of imaging (mean±SD, n=75 fields of view). **(E)** Images show control and ΔNp63 depleted SUM159O spheroids 72 h after plating in ECM. Scale bars, 100 μm. **(F)** Quantification shows the mean displacement of cells in control and p63 shRNA expressing SUM159O spheroids analyzed in **Fig. 2C-D**. Mean ± SD cell speed for 16 spheroids (Control) and 12 spheroids (p63 shRNA). **(G)** Quantification showing how p63 shRNA expression influences the mean speed of SUM159O cells grown in 2D monolayers over at least 6 h of imaging (mean±SD, n=75 fields of view). P-values determined by two-tailed Student's t-test **(F-G)** or Mann-Whitney U test **(A, C, D)**.

Figure S3

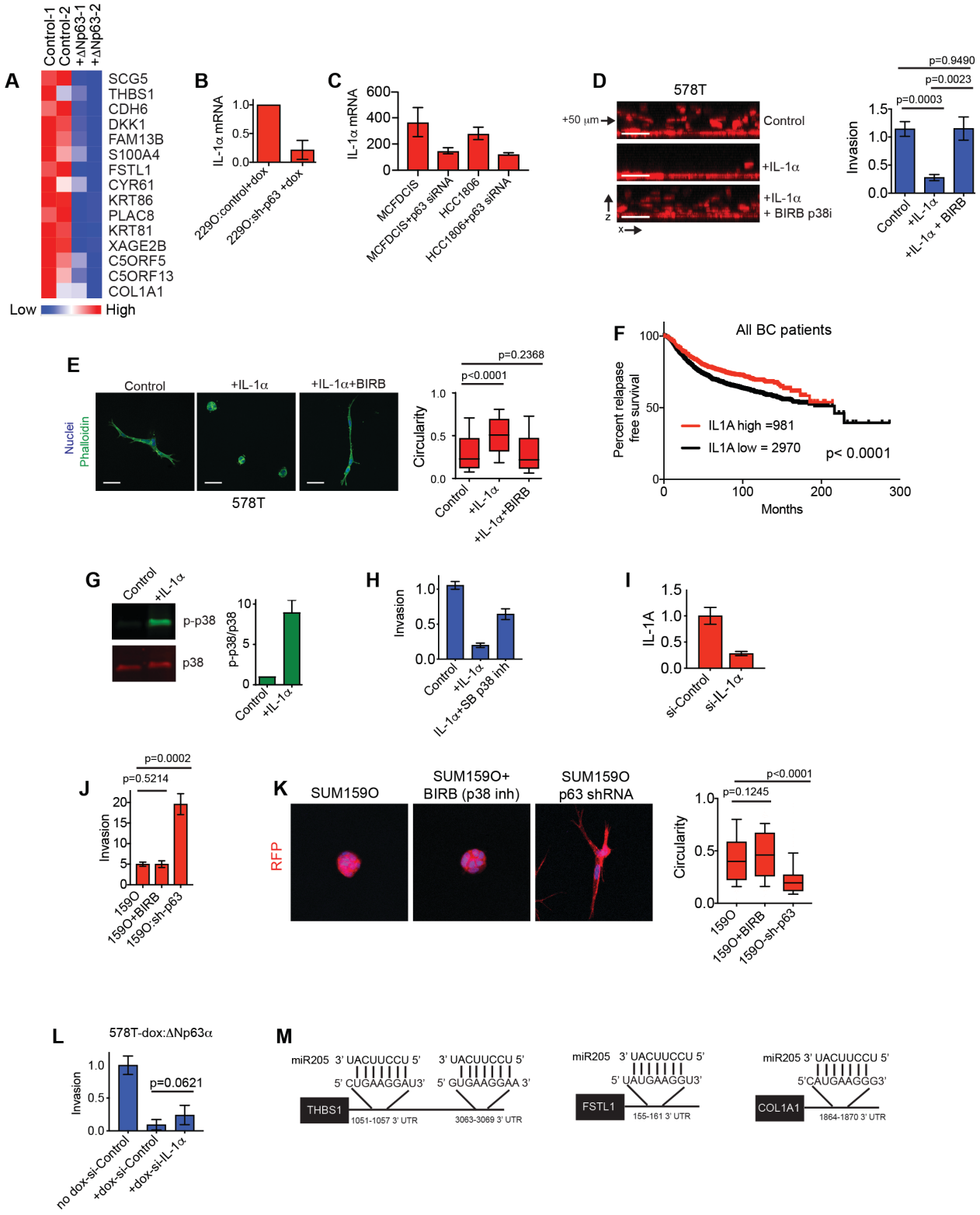
A
Control-1
Control-2
+ΔNp63-1
+ΔNp63-2
SCG5
THBS1
CDH6
DKK1
FAM13B
S100A4
FSTL1
CYR61
KRT86
PLAC8
KRT81
XAGE2B
C5ORF5
C5ORF13
COL1A1
Low
High
B
IL-1α mRNA
229O:control+dox
229O:sh-p63 +dox
C
IL-1α mRNA
MCFDCIS
MCFDCIS+p63 siRNA
HCC1806
HCC1806+p63 siRNA
D
578T
+50 μm
Control
+IL-1α
+IL-1α
+ BIRB p38i
z
x
p=0.9490
p=0.0023
p=0.0003
Invasion
Control
+IL-1α
+IL-1α + BIRB
E
Control
+IL-1α
+IL-1α+BIRB
Nuclei
Phalloidin
578T
p=0.2368
p<0.0001
Circularity
Control
+IL-1α
+IL-1α+BIRB
F
All BC patients
Percent relapse free survival
IL1A high =981
IL1A low = 2970
p< 0.0001
Months
G
Control
+IL-1α
p-p38
p38
p-p38/p38
Control
+IL-1α
H
Invasion
Control
+IL-1α
IL-1α+SB p38 inh
I
IL-1A
si-Control
si-IL-1α
J
p=0.0002
p=0.5214
Invasion
159O
159O+BIRB
159O:sh-p63
K
SUM159O
SUM159O+ BIRB (p38 inh)
SUM159O p63 shRNA
RFP
p<0.0001
p=0.1245
Circularity
159O
159O+BIRB
159O-sh-p63
L
578T-dox:ΔNp63α
p=0.0621
Invasion
no dox-si-Control
+dox-si-Control
+dox-si-IL-1α
M
miR205 3' UACUUCCU 5'
5' CUGAAGGAU3'
3' UACUUCCU 5'
5' GUGAAGGAA 3'
THBS1
1051-1057 3' UTR
3063-3069 3' UTR
miR205 3' UACUUCCU 5'
5' UAUGAAGGU3'
FSTL1
155-161 3' UTR
miR205 3' UACUUCCU 5'
5'CAUGAAGGG3'
COL1A1
1864-1870 3' UTR

Figure S3. (A) Heatmap showing the expression of 15 genes that were decreased at least 2-fold in SUM159T cells following 5 days of ΔNp63 induction. Biological replicates are shown. **(B)** Graph showing how p63 shRNA expression influences IL-1α levels in SUM229O cells (mean±range, n=2). **(C)** IL-1α mRNA expression in MCFDCISO and HCC1806 cells following transfection with control or p63 siRNA pools, as determined by microarray. Mean±range (n=2). **(D)** x-z projections and quantification showing how IL-1α [10 ng/ml] influences 578T invasion. The p38 inhibitor BIRB796 [1 μM] was included at the time of IL-1α treatment where indicated. Arrow is 50 μm above the monolayer and indicates invading cells (mean±SD, n=5).. Scale bars, 50 μm. **(E)** Images and quantification showing how IL-1α [10 ng/ml] influences the invasion of 578T cells 72 h after plating on ECM. The p38 inhibitor BIRB796 [1 μM] was included at the time of IL-1α treatment where indicated. Scale bars, 50 μm. Box and whisker plot (10-90 percentile). Control (n=1452), +IL-1α (n=1371) and +IL-1α+BIRB (n=1324 spheroids). **(F)** Kaplan-Meier curves showing relapse-free survival of breast cancer patients classified as "IL-1α-high" (red line) and "IL-1α-low" (black line) based on IL-1α mRNA expression using KM plotter. **(G)** Immunoblot showing total p38 MAPK and phospho-p38 MAPK levels following 15 min treatment with IL-1α [10 ng/ml] (mean+SD, n=3). **(H)** Quantification showing how the p38 inhibitor SB203580 [1 μM] influences the IL-1α dependent suppression of Hs578T invasion (mean±range, n=2). **(I)** Graph showing how transfection with an IL-1α siRNA pool influences IL-1α expression in SUM159O cells (mean±range, n=2). **(J)** Graph shows how the p38 inhibitor BIRB796 [10 μM] influences the vertical invasion of SUM159O cells (mean±SD, n=8). **(K)** Images and quantification showing how the p38 inhibitor BIRB796 [10 μM] influences the phenotype of SUM159O cells plated onto a layer of ECM for 48 h. Scale bars, 50 μm. Box and whisker plots (10-90 percentile). Control (n=129 spheroids), +BIRB (n=138 spheroids) and sh-p63 (n=136 spheroids). **(L)** Depletion of IL-1α fails to restore invasive properties in 578T cells expressing dox induced ΔNp63 (mean±SD, n=6). **(M)** The location of predicted miR205 targeted seed sequences in THBS1, FSTL1 and COL1A1 determined on Targetscan. P-values were determined by two-tailed Student's t-test **(D, L)** or Mann-Whitney U test **(E, J, K)**. Survival differences in **F** were compared using the log-rank (Mantel-Cox) test.

Figure S4

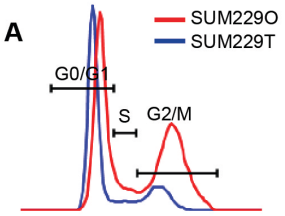

Cell Line	% G0/G1 phase	% S phase	% G2/M phase
SUM229O	38.9	17.7	43.5
SUM229T	64	15.6	20.4

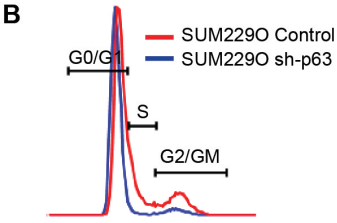

Cell Line	% G0/G1 phase	% S phase	% G2/M phase
SUM229O Control	62.4	22.4	15.1
SUM229O sh-p63	88.7	4.5	6.9

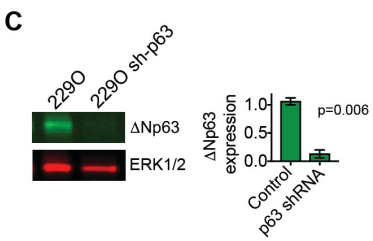

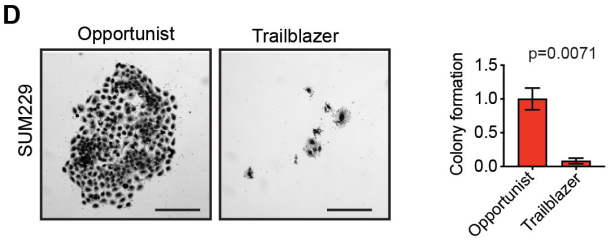

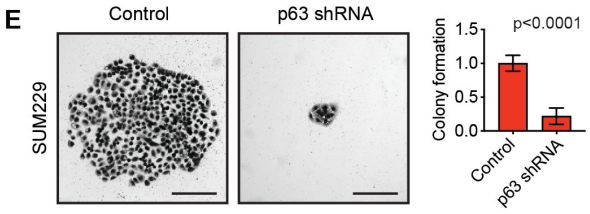

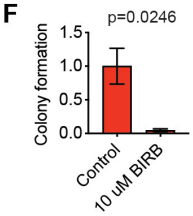

Figure S4. (A) Cell cycle analysis by flow cytometry of SUM229O and SUM229T cells. Tables show percentage of live cells in each cell cycle phase from a representative experiment (n=2). **(B)** Cell cycle analysis by flow cytometry of SUM229O cells stably expressing control or p63 shRNAs. Tables show percentage of live cells in each cell cycle phase from a representative experiment (n=2). **(C)** ΔNp63 expression in SUM229O cells stably expressing control or p63 shRNA (mean±SD, n=3)**. (D)** Colony formation by SUM229T and SUM229O cells (mean±SD, n=3). Scale bars, 200 µm. **(E)** Colony formation by SUM229O and SUM229O:sh-p63 cells (mean±SD, n=6). Scale bars, 200 µm. **(F)** Colony formation by SUM229O cells treated with 10 µM of the p38 inhibitor BIRB796 (mean±SD, n=3). Scale bars, 200 µm. P-values determined by two-tailed Student's t-test.

Figure S5

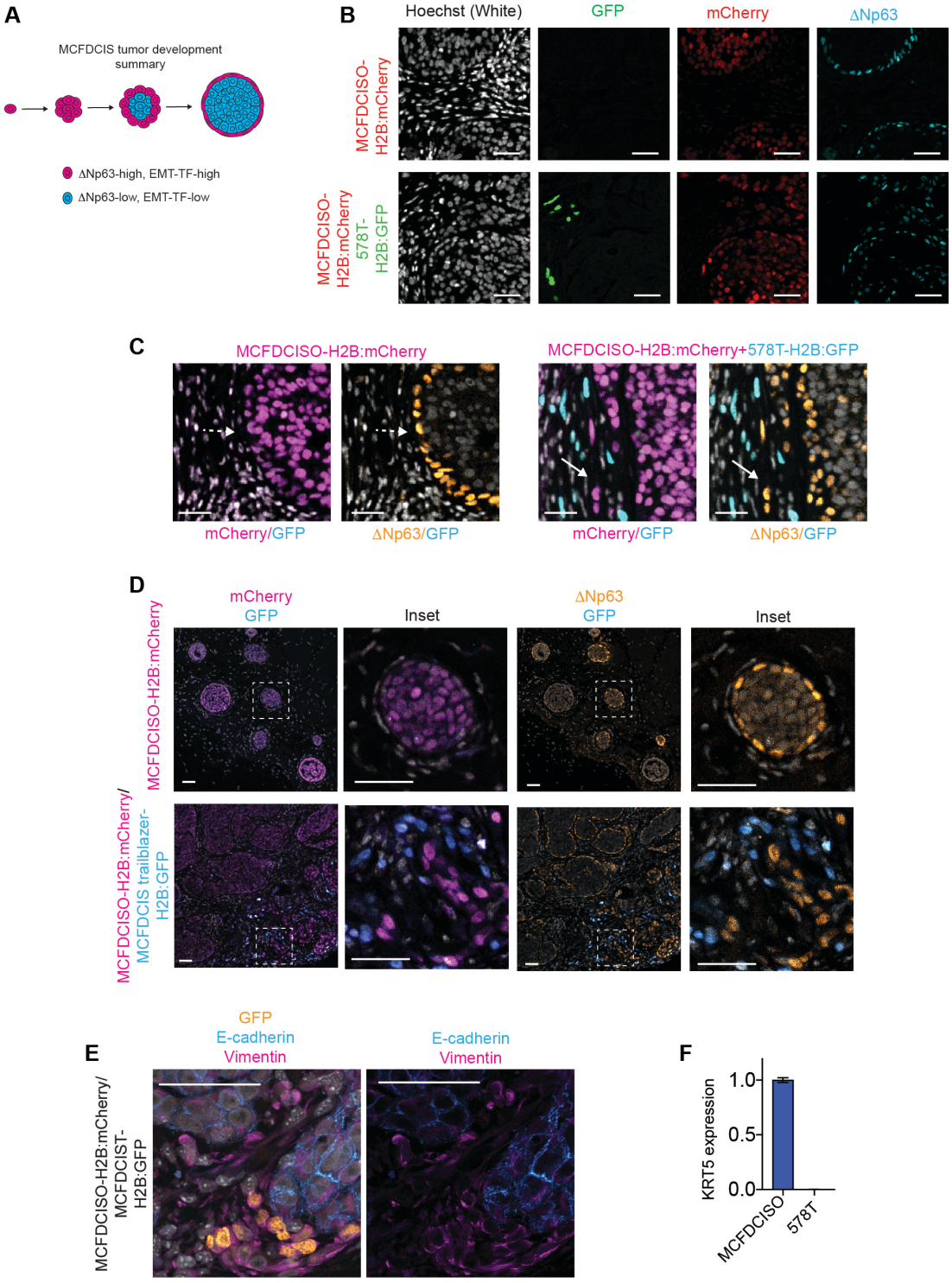
A
MCFDCIS tumor development summary
ΔNp63-high, EMT-TF-high
ΔNp63-low, EMT-TF-low
B
Hoechst (White)
GFP
mCherry
ΔNp63
MCFDCISO-H2B:mCherry
MCFDCISO-H2B:mCherry 578T-H2B:GFP
C
MCFDCISO-H2B:mCherry
MCFDCISO-H2B:mCherry+578T-H2B:GFP
mCherry/GFP
ΔNp63/GFP
mCherry/GFP
ΔNp63/GFP
D
mCherry
GFP
Inset
ΔNp63
GFP
Inset
MCFDCISO-H2B:mCherry
MCFDCISO-H2B:mCherry/ MCFDCIS trailblazer-H2B:GFP
E
GFP
E-cadherin
Vimentin
E-cadherin
Vimentin
MCFDCISO-H2B:mCherry/ MCFDCIST-H2B:GFP
F
KRT5 expression
1.0
0.5
0.0
MCFDCISO
578T

Figure S5. (A) Model summarizing the bi-potential nature of MCFDCISO cells when injected into the mammary fatpad of immune-compromised mice. The population injected expresses ΔNp63 and is in a ΔNp63-high EMT state. During the formation of tumor lesions the central luminal cells lose contact with the ECM and ΔNp63 expression is reduced. These cells do not express EMT-TFs and enter a static epithelial state. The ΔNp63 expressing cells adopt a myoepithelial phenotype based on the induction of SMA expression. Thus, the tumors have hallmark features of human DCIS. **(B)** Single color channel images corresponding to **Fig. 5A.** Scale bars, 50 µm. **(C)** Images show immunostaining of primary tumors composed of MCFDCISO cells alone or a mixture of MCFDCISO and 578T trailblazer cells (1:5 ratio) with GFP, mCherry and ΔNp63 antibodies. Solid arrows indicate representative areas of opportunistic collective invasion. Dashed arrows indicate a noninvasive tumor-ECM boundary (n=5 mice per condition). Scale bars, 50 µm. **(D)** Immunostaining of primary tumors composed of MCFDCISO cells alone or a mixture of MCFDCISO and MCFDCIST cells (1:10 ratio) using GFP, mCherry and ΔNp63 antibodies. Solid arrows indicate representative areas of opportunistic collective invasion. Dashed arrows indicate a noninvasive tumor-ECM boundary (n=5 mice per condition). Scale bars, 50 µm. **(E)** Representative immunostaining of MCFDCISO/MCFDCIST primary tumors using GFP, vimentin and E-cadherin antibodies. Scale bars, 50 µm. **(F)** KRT5 mRNA expression in MCFDCISO and 578T cells in culture, as determined by microarray (mean±range, n=2).

Video S1. Live imaging of clustered spheroids containing SUM159T-dox:ΔNp63 cells ± doxycycline (H2B:GFP, green, nuclei) showing cell motility. Fluorescent and bright field images were acquired at 20 min intervals over a span of 13 h. This is the time lapse imaging of the clustered SUM159-T-dox: ΔNp63 cells ± doxycycline shown in **Fig. 2A**. Scale bars, 50 μm.

Video S2. Live imaging of the inset region of clustered spheroids containing SUM159T-dox:ΔNp63 cells ± doxycycline (H2B:GFP, green, nuclei) showing cell motility. Fluorescent and bright field images were acquired at 20 min intervals over a span of 13 h. This is the time lapse imaging of the inset region shown in **Fig. 2A**. Scale bars, 50 μm.

Video S3. Live imaging of SUM159T cells embedded in ECM containing fluorescent microbeads (blue) showing ECM reorganization through bead movement. Fluorescent and bright field images were acquired at 15 min intervals over a span of 20 h. This is the time lapse imaging of the SUM159T cells and fluorescent microbeads shown in **Fig. S2A**. Scale bars, 50 μm.

Video S4. Live imaging of SUM159O cells embedded in ECM containing fluorescent microbeads (blue) showing ECM reorganization through bead movement. Fluorescent and bright field images were acquired at 15 min intervals over a span of 20 h. This is the time lapse imaging of the SUM159O cells and fluorescent microbeads shown **Fig. S2A**. Scale bars, 50 μm.

Video S5. Live imaging of clustered spheroids containing SUM159O cells expressing control or a p63 shRNA (H2B:mCherry, red, nuclei) showing cell motility. Fluorescent and bright field images were acquired at 25 min intervals over a span of 13 h. This is the time lapse imaging of clustered SUM159O:sh-Control and SUM159O:sh-p63 cells shown in **Fig. 2C**. Scale bars, 50 μm.

Video S6. Live imaging of the inset region of clustered spheroids containing SUM159O cells expressing control or a p63 shRNA (H2B:mCherry, red, nuclei) showing cell motility. Fluorescent and bright field images were acquired at 25 min intervals over a span of 13 h. This is the time lapse imaging of the inset regions shown in **Fig. 2C**. Scale bars, 50 μm.

Video S7. Live imaging of explants containing MCFDCISO cells (H2B:mCherry, red, nuclei) with or without 578T cells (H2B:GFP, green, nuclei) showing cell motility. Fluorescent and bright field images were acquired at 45 min intervals over a span of 21 h. This is the time lapse imaging of the tumor explants composed of MCFDCISO cells alone or a mixture of MCFDCISO and 578T cells (1:5 ratio) shown in **Fig. 5D**. Scale bars, 50 μm.

Table S1. Description of the cell lines used in the study. Cell line names, invasive phenotype, method of derivation and E-cadherin status are indicated.

Table S2. Genes expressed at a higher level in SUM159 opportunist cells relative to SUM159 trailblazer cells. Genes that were at least 4-fold higher in opportunist cells relative to trailblazer cells with a false discovery rate (FDR) of <0.01.

Table S3. Genes induced by doxycycline induced ΔNp63 expression in SUM159 trailblazer cells. Genes that were at least 2-fold increased in expression in SUM159 trailblazer cells 5 days after doxycycline induced ΔNp63 expression.

Table S4. Genes suppressed by doxycycline induced ΔNp63 expression in SUM159 trailblazer cells. Genes that were at least 2-fold decreased in SUM159 trailblazer cells 5 days after doxycycline induced ΔNp63 expression.

Table S5. MMP expression in control and ΔNp63 expressing SUM159 trailblazer cells. MMP expression in SUM159 trailblazer cells 5 days after doxycycline induced ΔNp63 expression.

Table S6. List of antibodies used for each mode of analysis.

Table S7. Targeting sequences of siRNAs and shRNAs.

Table S8. List of primers used for qPCR.